Medicine®

OBSERVATIONAL STUDY

OPEN

Intravoxel Incoherent Motion MR Imaging: Comparison of Diffusion and Perfusion Characteristics for Differential Diagnosis of Soft Tissue Tumors

Jun Du, MD, Kun Li, MD, Weisheng Zhang, MD, PhD, Shaowu Wang, MD, PhD, Qingwei Song, MD, Ailian Liu, MD, PhD, Yanwei Miao, MD, PhD, Zhijin Lang, MD, Lina Zhang, MD, and Minting Zheng, MD

Abstract: We used intravoxel incoherent motion (IVIM) magnetic resonance imaging (MRI) to explore the possibility of preoperative diagnosis of soft tissue tumors (STTs). This prospective study enrolled 23 patients. Conventional MRI and IVIM examinations were performed on a 3.0T MR imager. Eight (35%) hemangiomas, 11 (47%) benign soft tissue tumors excluding hemangiomas (BSTTEHs) and 4 soft tissue sarcomas (STSs) were assessed. The mean tumor size was about $1652.36 \pm 233.66\,mm^2$. Ten b values ($0–800\,s/mm^2$) were used to evaluate diffusion and perfusion characteristics of IVIM. IVIM parameters ($ADC_{standard}$, ADC_{slow}, ADC_{fast}, and f) of STTs were measured and evaluated for differentiating hemangiomas, BSTTEHs, and STSs. ADC_{slow} and ADC_{fast} value were different for hemangiomas, BSTTEHs, and STSs separately ($P < 0.001$, $P < 0.001$, and $P = 0.001$). ADC_{slow}, cut-off value smaller than $0.93 \times 10^{-3}\,mm^2/s$, was the best parameter to differ STSs ($0.689 \pm 0.173 \times 10^{-3}\,mm^2/s$) from hemangiomas ($0.933 \pm 0.237 \times 10^{-3}\,mm^2/s$) and BSTTEHs ($1.156 \pm 0.120 \times 10^{-3}\,mm^2/s$) ($P = 0.001$). ADC_{slow} ($0.93 \times 10^{-3}\,mm^2/s$ <cut-off value $<0.96 \times 10^{-3}\,mm^2/s$) was used to distinguish hemangiomas from BSTTs. There were significant difference among hemangiomas, BSTTEHs, and STSs ($P = 0.014$, $P = 0.036$, $P < 0.001$). The $ADC_{standard}$, ADC_{fast}, and f value were different ($P < 0.05$) for STSs ($1.009 \pm 0.177 \times 10^{-3}\,mm^2/s$, $15.700 \pm 1.992 \times 10^{-3}\,mm^2/s$, 0.503 ± 0.068), hemangiomas ($1.505 \pm 0.226 \times 10^{-3}\,mm^2/s$, $11.675 \pm 0.456 \times 10^{-3}\,mm^2/s$, 0.682 ± 0.060), and BSTTEHs ($1.555 \pm 0.176 \times 10^{-3}\,mm^2/s$, $11.727 \pm 0.686 \times 10^{-3}\,mm^2/s$, 0.675 ± 0.054). And there was no significant difference for these 3 parameters between hemangiomas and BSTTEHs ($P = 0.584$, 0.907, and 0.798). IVIM may be of significant value for differential diagnosing hemangiomas, BSTTEHs, and STSs.

(*Medicine* 94(25):e1028)

Abbreviations: ADC = apparent diffusion coefficient, BSTTEHs = benign soft tissue tumors excluding hemangiomas, BSTTs = benign soft tissue tumors, DWI = diffusion weighted imaging, MRI = magnetic resonance imaging, STSs = soft tissue sarcomas, STTs = soft tissue tumors.

INTRODUCTION

Soft tissue tumors (STTs), putatively mesenchymal origin, are sporadic without a known pathogenesis or established risk factors. There is a rising incidence in recent years for benign soft tissue tumors (BSTTs) more than 300/100,000 and malignant ones around 5/100,000 per year.[1] In addition, STTs represent a striking range of morphologic diversity and multiple individual clinical symptoms among different types.[2] Differential diagnosis of benign tumors and malignant ones should be made for further treatment in clinic. Soft tissue sarcomas (STSs), as the main malignant tumors, occur at any age and account for only 21% of all pediatric solid malignant cancers and less than 1% of all adult solid malignant cancers.[3] It is difficult to make a prospectively preoperative diagnosis of different subtypes of STTs due to their complexity and rarity.

Magnetic resonance imaging (MRI) is considered the first choice of imaging modality to evaluate STTs.[4] However, there still are lots of problems need to be dealt with. For example, BSTTs may achieve dedifferentiation and exhibit hybrid histologic characteristics of malignant propensity. In addition, hemangiomas, accounting for 7% of BSTTs,[5] show diffuse growth and easy to relapse, which is the main cause of clinical misdiagnosis as malignant tumor. It is reported that MR imaging cannot reliably distinguish benign and malignant lesions when radiologic evaluation is nonspecific.[6] The inhomogeneity of lesions on T_2, the change from homogeneity on T_1 to inhomogeneity on T_2 sequence, and the involvement of bone or neurovascular structures are features that may be helpful in differential diagnosing benign from malignant soft tissue masses, while whether MRI can be used to differentiate benign from malignant ones is still controversial.[7]

Intravoxel incoherent motion (IVIM) imaging is an extension of diffusion weighted imaging (DWI) that integrates the apparent diffusion coefficient (ADC) contains both perfusion and diffusion terms.[8] Diffusion and perfusion are physically and biologically different phenomena.[9] The diffusion property of tumor tissues largely depends on cell density, which may also be predictive features of malignancy in some types of tumors. Perfusion is an important phenomenon of many physiological or pathological processes.[8] It is reported that IVIM imaging may be helpful for differentiating benign and malignant salivary gland tumors.[10] Therefore, to estimate these 2 distinctive

Editor: Mariusz Adamek.
Received: March 22, 2015; revised: May 13, 2015; accepted: May 19, 2015.
From the Department of Radiology, First Affiliated Hospital of Dalian Medical University (JD, WZ, QS, AL, YM, ZL, LZ, MZ); Department of Radiology, Second Affiliated Hospital of Dalian Medical University (SW); and Department of orthopedics, Second Affiliated Hospital of Dalian Medical University, Dalian, China (KL).
Correspondence: Weisheng Zhang, Department of Radiology, First Affiliated Hospital of Dalian Medical University, Dalian 116011, China (e-mail: 11111210027@fudan.edu.cn).
Shaowu Wang, Department of Radiology, Second Affiliated Hospital of Dalian Medical University, Dalian 116023, China (e-mail: wsw_2003@163.com).
The authors have no funding and conflicts of interest to disclose.

ISSN: 0025-7974
DOI: 10.1097/MD.0000000000001028

TABLE 1. Primary Sites and Clinical Data of 23 Soft Tissue Tumors

			Sex			Primary Sites of STTs						
STTs	Proportion	NO.	F	M	Average Age	Shoulder and Back	Upper Arm	Forearm	Thigh	Knee	Shank	Ankle and Foot
Hemangiomas	35%	8	5	3	35			2	2	1	1	2
BSTTEHs	48%	11	4	7	51							
Desmoid-type fibromatosis		1					1					
Epidermoid cyst		1									1	
Lipoma		1									1	
Lymphangioma		1				1						
Proliferative myositis		1									1	
Schwannomas		5					1		1	3		
Tenosynovial giant cell tumour-localized type		1										1
STSs	17%	4	2	2	53							
Liposarcomas		3				2			1			
Extraskeletal myxoid chondrosarcoma		1									1	
Total	100%	23	11	12		3	2	2	4	4	5	3

BSTTEHs = benign soft tissue tumors excluding hemangiomas, F = female, M = male, NO. = the number of soft tissue tumors, STSs = soft tissue sarcomas, STTs = soft tissue tumors.

phenomena in tumor tissues may be helpful in the diagnosis of STTs before surgery.

The purpose of the present study was to assess the IVIM parameters for differential diagnosing hemangiomas, benign soft tissue tumors excluding hemangiomas (BSTTEHs), and STSs.

PATIENTS AND METHODS

Patients

The study was approved by the Institutional Ethics Committee of First Affiliated Hospital of Dalian Medical University (Dalian, China). Thirty-one consecutive patients were enrolled in this study and inspected conventional MR and IVIM-MR examination with 3.0-T MR imager from October 2013 to October 2014. Eight of these patients were excluded for further analysis: 4 patients did not receive surgery and there were no pathological results available; 1 tumor in the upper limb was close to artery and the quality of image was very poor; and for other 3 patients, there were no sufficient regions of interest (ROI) areas for IVIM analysis. As a result, only 23 STTs were further analyzed. Primary sites and clinical data of these tumors (11 female, 12 male; average age, 44 years; age range 16–85 years) were described in Table 1.

Conventional MR Imaging

MRI was performed using a 3.0-T MR imager (Signa, HDxt, 3.0 T; General Electric Healthcare, Milwaukee, WI) with surface coil (limbs with 3 inch coil, shoulder with shoulder coil or soft coil, and torso and hips with body coil). The conventional MR scanning sequences included spin echo (SE) T1WI (repetition time/echo time [TR/TE], 650 ms/min full; reconstruction matrix size, 288 × 224; slice thickness/slice spacing, 4–6 mm/0–1 mm), fast spin echo (FSE) T_2WI (TR/TE, 3975 ms/68 ms; number of signals acquired, 4; reconstruction matrix size, 256 × 224; slice thickness/slice spacing, 4–6 mm/0–1 mm), fat suppression T_2WI and PDWI (TR/TE, 2000 ms/42 ms; number of signals acquired, 3; reconstruction matrix size, 256 × 224; slice thickness/slice spacing, 4–6 mm/0–1 mm). If necessary, fat suppression T_1WI was performed. Field of view (FOV), which could be changed according to the tumors' size, was 15 to 40 cm with slice thickness 4 to 6 mm and space 0 to 1 mm.

IVIM MR Imaging

IVIM scan was performed using spin-echo echo-planar imaging (SE-EPI) sequence (TR/TE, 8000 ms/min; NEX, 8; reconstruction matrix size, 128 × 128; slice thickness, slice spacing, and FOV similar to conventional scan; 10 b values [0, 10, 20, 30, 50, 100, 200, 300, 500, and 800 s/mm^2]). In order to eliminate the influence of the anisotropy for the IVIM signal and the numerical measurement, 3 in 1 was applied. All patients were fixed on bed to prevent the influence of movement.

Based on IVIM theory, the bi-exponential model was expressed by the following equation:[11]

$$S_b/S_0 = (1 - f) \cdot \exp(-b \cdot ADC_{slow}) + f \cdot \exp[-b \cdot (ADC_{fast} + ADC_{slow})],$$

where S_b is the signal intensity in the pixel with diffusion gradient b, S_0 the signal intensity in the pixel without diffusion gradient (b of 0 s/mm^2), f the fractional perfusion related to the microcirculation, ADC_{slow} the true diffusion coefficient as reflected by pure molecular diffusion, and ADC_{fast} is the pseudo-diffusion coefficient representing perfusion-related diffusion or incoherent microcirculation.

TABLE 2. One-Way ANOVA Tests Differing IVIM Parameters Among Hemangiomas, BSTTEHs, and STSs

	$ADC_{standard}$ ($\times 10^{-3}$ mm^2/s)	ADC_{slow} ($\times 10^{-3}$ mm^2/s)	ADC_{fast} ($\times 10^{-3}$ mm^2/s)	f
Hemangiomas (n = 8)	1.505 ± 0.226	0.933 ± 0.237	11.675 ± 0.456	0.682 ± 0.060
BSTTEHs (n = 11)	1.555 ± 0.176	1.156 ± 0.120	11.727 ± 0.686	0.675 ± 0.054
STSs (n = 4)	1.009 ± 0.177	0.689 ± 0.173	15.700 ± 1.992	0.503 ± 0.068
P value	< 0.001	0.001	< 0.001	< 0.001

BSTTEHs = benign soft tissue tumors excluding hemangiomas, IVIM = intravoxel incoherent motion, STSs = soft tissue sarcomas.

Dynamic Contrast-Enhanced MR Imaging

Dynamic contrast-enhanced MR imaging was performed using 2-dimensional fast spoiled gradient echo sequence (2D FSPGR). The contrast agent gadolinium-DTPA (Magnevist, Berlex, New Jersey) was injected as 0.1 mmol/kg, and 2.5 mL/s. And 10 mL saline was additionally injected at the same velocity.

Regions of Interest (ROI)

ROI was placed on the parenchyma of each tumor in DWI. Large cystic or necrotic areas and large vessels were not included. The mean ROI area was about 15.0 ± 1.21 mm^2. Three ROIs in each image and totally 9 ROIs in 3 consecutive images of IVIM were calculated for each patient. The different values ($ADC_{standard}$, ADC_{slow}, ADC_{fast}, and f) of STTs were measured in GE-ADW 4.4 workstation.

Statistical Analysis

Two independent-sample *t*-test was used for assessing ADC_{slow} and ADC_{fast} of hemangiomas, BSTTEHs, and STSs separately. One-way ANOVA and least significant difference (LSD) *t*-test were used for comparing IVIM parameters among the 3 types of STTs. Receiver operating characteristic (ROC) curves were generated with respective cut-off values determined to accommodate best diagnostic accuracy based on the Youden index. SPSS (version19.0, Chicago, IL) was used for statistical analysis. *P* values < 0.05 were considered significant for 2-tailed probability.

RESULTS

In total, ROIs from 8 hemangiomas, 11 BSTTEHs, and 4 STSs were evaluated. The mean tumor size (maximum tumor areas measured using axial contrast-enhanced MR images) was 1652.36 ± 233.66 mm^2. ADC_{slow} and ADC_{fast} value were different among hemangiomas, BSTTEHs, and STSs separately ($P < 0.001$, $P < 0.001$, and $P = 0.001$).

Each IVIM parameter ($ADC_{standard}$, ADC_{slow}, ADC_{fast}, and f) for STTs was significant difference ($P < 0.001$, $P = 0.001$, $P < 0.001$, and $P < 0.001$) (Table 2, Figures 3–5). Multiple comparisons of IVIM parameters between each index are summarized in Table 3. The $ADC_{standard}$, ADC_{fast}, and f values of hemangiomas and STSs or BSTTEHs and STSs were significant difference ($P < 0.05$), while there was no significant difference for these 3 parameters between hemangiomas and BSTTEHs ($P = 0.584$, $P = 0.907$, and $P = 0.798$). The ADC_{slow} values between hemangiomas and BSTTEHs, hemangiomas and STSs, and also BSTTEHs and STSs were significant difference ($P = 0.014$, $P = 0.036$, and $P < 0.001$).

The ROC curves and optimal cut-off values of IVIM parameters were used to identify STSs from STTs (Figure 1 and Table 4). The ADC_{slow} value was the most powerful parameter, with area under the curve of 0.86, followed by $ADC_{standard}$ 0.72 and f 0.56. ADC_{fast} was the least meaningful one with area 0.34. The ROC curve and optimal cut-off value of ADC_{slow} were used to discriminate hemangiomas from BSTTs in Figure 2 and Table 5. The optimal cut-off value was between 0.93×10^{-3} and 0.96×10^{-3} mm^2/s. Two steps to deal with STTs were indicated in Table 6. First step was to separate BSTTs (Figures 3 and 4) from STSs (Figure 5), and then to identify hemangiomas (Figure 3) from BSTTs.

DISCUSSION

There are similar imaging characteristics (such as diffuse growth, easy to relapse, and high signal intensity on T_2-weighted imaging/DW-MRI) for hemangiomas and malignant tumors. This is the main reason for radiological and clinical misdiagnosing hemangiomas as malignant tumors. So hemangiomas were classified out as a separate group in this study.

IVIM MR imaging has been utilized as an attractive noninvasive imaging technique with the potential for assessing both tissue perfusion and diffusion of STTs using a single DW imaging.[10,12] And it shows a unique profile of microcirculation and pure molecular diffusion within tumors. Our study showed that the ADC_{slow} and ADC_{fast} values of hemangiomas, BSTTEHs, and STSs were significantly different, which suggested that IVIM imaging facilitates understanding of tumor tissue characteristics of perfusion and diffusion.

On the other hand, $ADC_{standard}$ values of hemangiomas, BSTTEHs, and STSs were also significantly different. The $ADC_{standard}$ of BSTTEHs was maximum ($1.555 \pm 0.176 \times 10^{-3}$ mm^2/s), while the $ADC_{standard}$ of STSs was minimum ($1.009 \pm 0.177 \times 10^{-3}$ mm^2/s) due to active proliferative capacity of sarcomas. The limitation of water molecular diffusion of malignant tumors leads to the decrease of ADC value.[13]

In the bi-exponential model, ADC_{slow} ($P = 0.014$) was an effective parameter to distinguish hemangiomas from other benign tumors. ADC_{slow} with a high b value (>200 s/mm^2) is the true diffusion coefficient of pure water in tumors with perfusion components removed at the same time. There were significant differences for values of ADC_{slow} among hemangiomas, BSTTEHs, and STSs (Table 3). The value of ADC_{slow} decreased from BSTTEHs to STSs with hemangiomas in the

TABLE 3. LSD *t*-tests of Multiple Comparison of IVIM Parameters Value Among Hemangiomas, BSTTEHs, and STSs

Dependent Variable	LSD *t*-tests	*P* Value
$ADC_{standard}$ ($\times 10^{-3}$ mm^2/s)	Hemangiomas vs BSTTEHs	0.584
	Hemangiomas vs STSs	<0.001
	BSTTEHs vs STSs	<0.001
ADC_{slow} ($\times 10^{-3}$ mm^2/s)	Hemangiomas vs BSTTEHs	0.014
	Hemangiomas vs STSs	0.036
	BSTTEHs vs STSs	<0.001
ADC_{fast} ($\times 10^{-3}$ mm^2/s)	Hemangiomas vs BSTTEHs	0.907
	Hemangiomas vs STSs	<0.001
	BSTTEHs vs STSs	<0.001
F	Hemangiomas vs BSTTEHs	0.798
	Hemangiomas vs STSs	<0.001
	BSTTEHs vs STSs	<0.001

BSTTEHs = benign soft tissue tumors excluding hemangiomas, IVIM = intravoxel incoherent motion, LSD = least significant difference, STSs = soft tissue sarcomas, vs = versus.

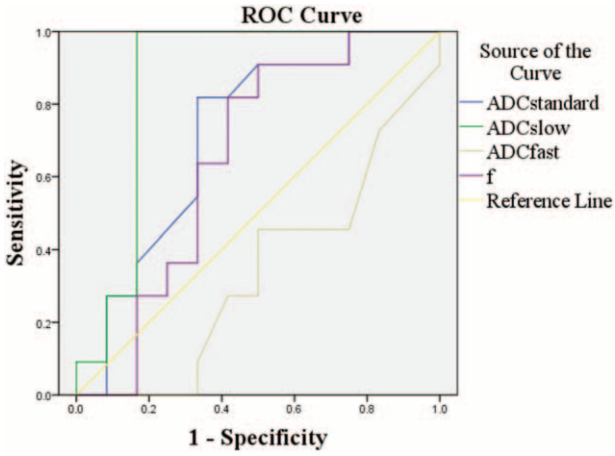

FIGURE 1. ROC curves of IVIM parameters for identifying soft tissue sarcoma from hemangioma and benign tumors.

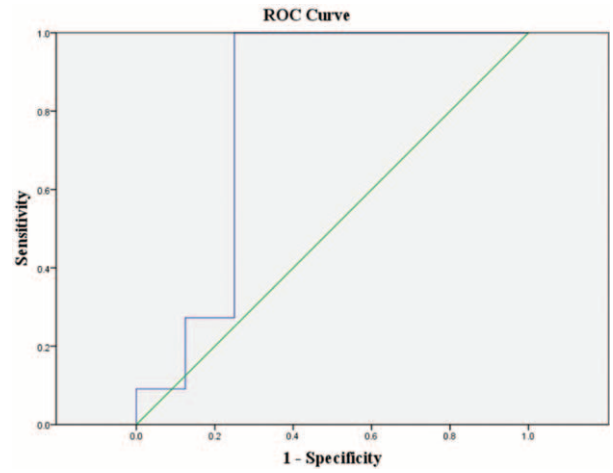

FIGURE 2. ROC curve of ADC_{slow} for discriminating hemangioma from benign tumors.

TABLE 4. Diagnostic Characteristics of IVIM Parameters to Identify STSs From STTs Based on the Respective Cut-Off Values

	Cut-off Value	Sensitivity, %	Specificity, %	Accuracy, %	95% Confidence Interval
$ADC_{standard}$ ($\times 10^{-3}$ mm^2/s)	<1.44	82	67	72	0.50–0.93
ADC_{slow} ($\times 10^{-3}$ mm^2/s)	<0.93	100	83	86	0.69–1.00
ADC_{fast} ($\times 10^{-3}$ mm^2/s)	>11.75	46	50	34	0.11–0.56
F	<0.64	82	58	65	0.42–0.89

STSs = soft tissue sarcomas, STTs = soft tissue tumors.

TABLE 5. Diagnostic Characteristics of ADC_{slow} to Discriminate Hemangiomas from BSTTs Based on the Respective Cut-Off Values

	Cut-Off Value	Sensitivity, %	Specificity, %	Accuracy, %	95% Confidence Interval
ADC_{slow} ($\times 10^{-3}$ mm^2/s)	<0.96	100	75	80	0.54–1.00

BSTTs = benign soft tissue tumors.

middle level. The reason is that potential proliferation of STSs is faster than BSTTs. For STSs, there are large nuclei, less cytoplasm, and a dense array of cells, which lead to the extracellular space reduced, the cell membrane permeability reduced, and the water molecular diffusion limited.[14–17] So ADC_{slow} decreased significantly. According to ROC curve, the cut-off value of ADC_{slow} without perfusion effects is smaller than that of $ADC_{standard}$ in the bi-exponential of IVIM model. As stated above, ADC_{slow} may be a meaningful parameter for differential diagnosis of hemangiomas, BSTTEHs, and STSs.

Microcirculation perfusion, namely fast moving component in the bi-exponential of IVIM model, is more sensitive to the MR signal attenuation.[18] According to the bi-exponential theory, ADC_{fast} is closely related to microvessel density of tumor tissues at low b value (<200 s/mm^2). In this study, ADC_{fast} was significantly greater than related ADC_{slow}. It means that ADC_{fast} is sensitive to MR signal attenuation at lower b values. There is a maximum value of ADC_{fast} of STSs as the same results of report[12] about ADC_{fast} for different groups (cervical tumor, myometrium, and leiomyoma), which confirmed ADC_{fast} associated with the degree of tissue microvessel perfusion.

The fractional volume of capillary blood flowing in each voxel is measured using f.[19] f value may correlate with the amount of normal angiogenesis with intact vessels in terms of basement membrane thickness and pericyte coverage, and it increases with the augmented tissue perfusion components.[20] Our results suggest that hemangiomas (0.682 ± 0.060) are rich in capillaries per unit tumor volume, while STSs (0.503 ± 0.068) are relatively poor in capillaries because liposarcomas and extraskeletal myxoid chondrosarcomas are not rich in blood vessels. Therefore, f value may be an indicator of intact vascular permeability.

TABLE 6. Two Steps to Deal with STTs: Firstly, Differentiating BSTTs and STSs, and Then Identifying Hemangiomas From BSTTs

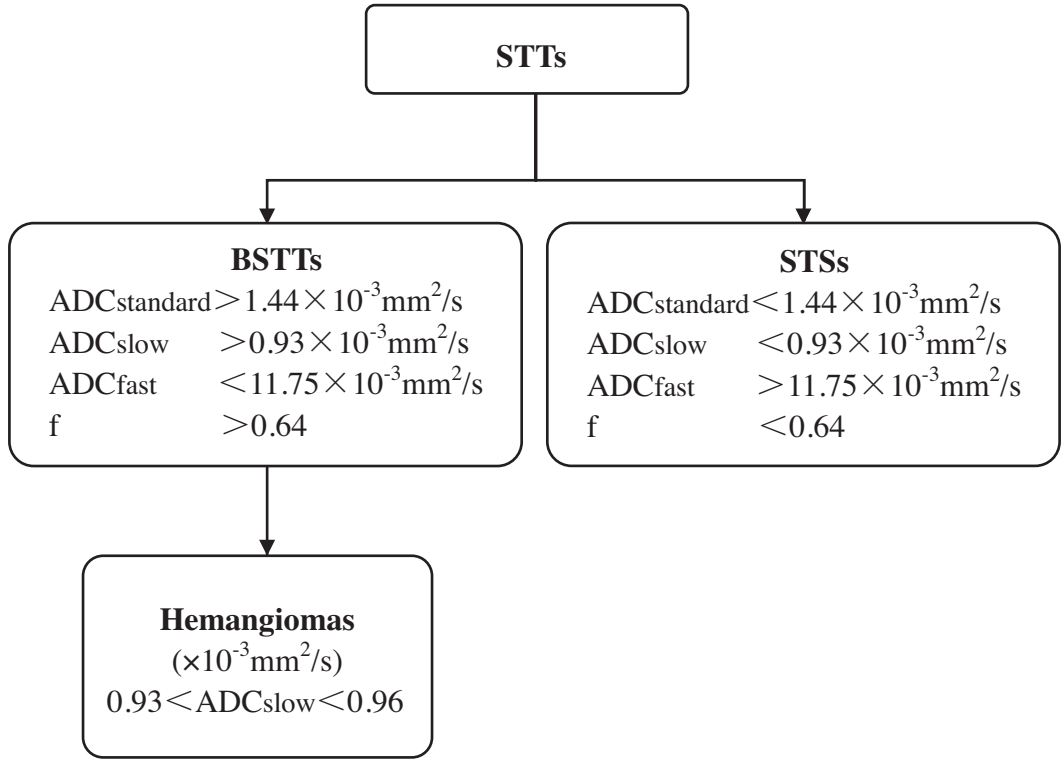

BSTTs = benign soft tissue tumors, STSs = soft tissue sarcomas, STTs = soft tissue tumors.

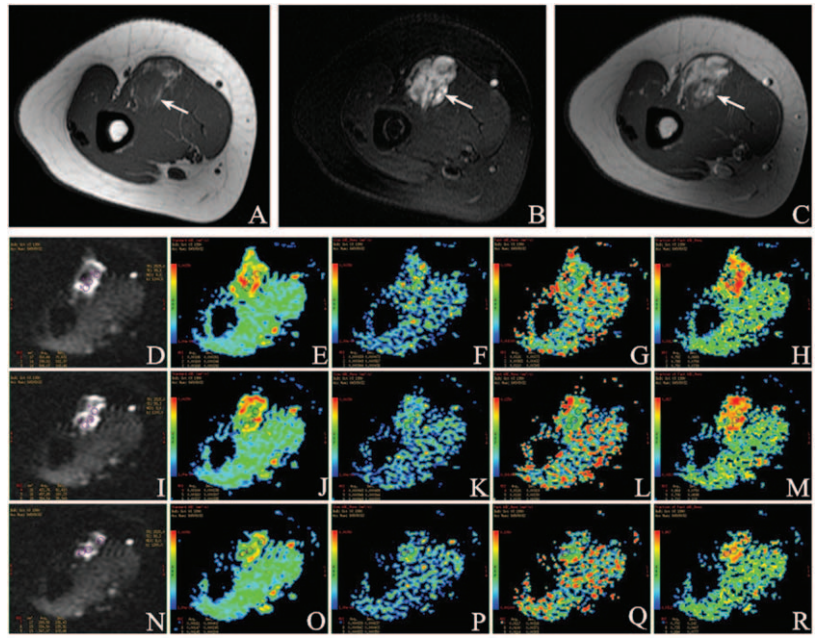

FIGURE 3. A 23-year-old female was diagnosed hemangioma (arrow) in the right brachialis. (A) Axial T_1WI demonstrates a solid mass of intermediate signal intensity (SI) compared to adjacent muscles. (B) Axial T_2WI shows a lobulated mass with high SI. (C) Contrast-enhanced T_1WI image shows intense homogeneous enhancement with large internal vessels. Characteristic changes in intravoxel incoherent motion (IVIM) parameters: (D) Location maps of ROI_1, ROI_2, and ROI_3 in the first sectional image. Images (E–H) show $ADC_{standard}$, ADC_{slow}, ADC_{fast}, and f value separately. (I) Location maps of ROI_4, ROI_5, and ROI_6 in the second sectional image. $ADC_{standard}$, ADC_{slow}, ADC_{fast}, and f value were placed in (J–M) successively. (N) Location maps of ROI_7, ROI_8, and ROI_9 in the third sectional image. $ADC_{standard}$, ADC_{slow}, ADC_{fast}, and f value were put in (O–R) in proper order. Mean value of $ADC_{standard}$ is $0.00160 \pm 0.000288\,mm^2/s$, ADC_{slow} $0.000943 \pm 0.000448\,mm^2/s$, ADC_{fast} $0.0111 \pm 0.00319\,mm^2/s$, and f 0.725 ± 0.0827 from ROI_1 to ROI_9, accordingly.

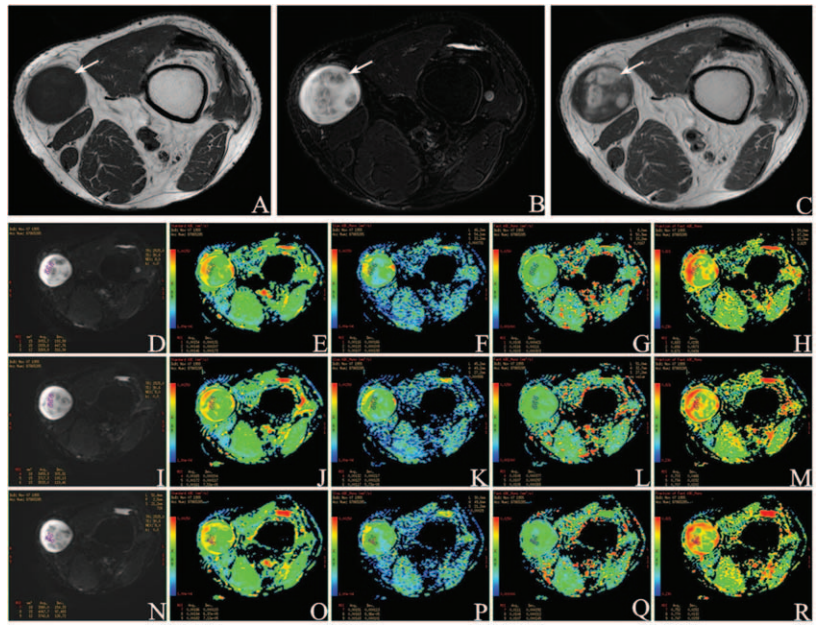

FIGURE 4. A 59-year-old male was diagnosed Schwannoma (arrow) in the subcutaneous fat of left knee between vastus medialis and sartorius. (A) Axial T_1WI demonstrates a solid mass of intermediate signal intensity (SI). (B) Axial T_2WI shows the ovoid mass with heterogeneously hyper SI. (C) Contrast-enhanced T_1WI shows heterogeneously enhanced. Characteristic changes in IVIM parameters: (D) Location map of ROI_1, ROI_2, and ROI_3 in the first sectional image. Images (E–H) separately show $ADC_{standard}$, ADC_{slow}, ADC_{fast}, and f value. (I) Location map of ROI_4, ROI_5, and ROI_6 in the second sectional image. $ADC_{standard}$, ADC_{slow}, ADC_{fast}, and f value were placed in (J–M) successively. (N) Location maps of ROI_7, ROI_8, and ROI_9 in the third sectional image. $ADC_{standard}$, ADC_{slow}, ADC_{fast}, and f value were put in (O–R) in proper order. Mean value of $ADC_{standard}$ is $0.00168 \pm 0.000129\,mm^2/s$, ADC_{slow} $0.00130 \pm 0.000140\,mm^2/s$, ADC_{fast} $0.0108 \pm 0.000380\,mm^2/s$, and f 0.714 ± 0.0307 from ROI_1 to ROI_9, accordingly.

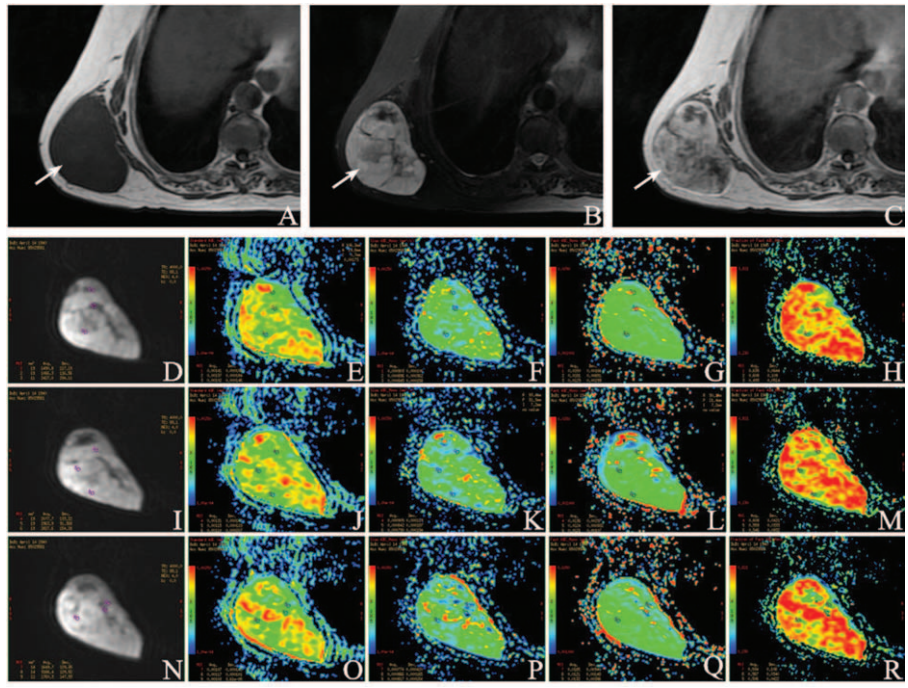

FIGURE 5. A 74-year-old female was diagnosed myxoid liposarcoma (arrow) in the subcutaneous fat of her right back. (A) Axial T_1WI demonstrates a solid mass of low signal intensity (SI). (B) Axial T_2WI shows a lobulated mass with high SI. (C) Contrast-enhanced T_1WI shows heterogeneously enhanced solid tissues and thickened septa. Characteristic changes in IVIM parameters: (D) Location maps of ROI_1, ROI_2, and ROI_3 in the first sectional image. Images (E–H) separately show $ADC_{standard}$, ADC_{slow}, ADC_{fast}, and f value. (I) Location maps of ROI_4, ROI_5, and ROI_6 in the second sectional image. $ADC_{standard}$, ADC_{slow}, ADC_{fast}, and f value were placed in (J–M) successively. (N) Location maps of ROI_7, ROI_8, and ROI_9 in the third sectional image. $ADC_{standard}$, ADC_{slow}, ADC_{fast}, and f value were put in (O–R) in proper order. Mean value of $ADC_{standard}$ is $0.00118 \pm 0.000134\ mm^2/s$, ADC_{slow} $0.000849 \pm 0.000207\ mm^2/s$, ADC_{fast} $0.0140 \pm 0.00344\ mm^2/s$, and f 0.562 ± 0.0631 from ROI_1 to ROI_9, accordingly.

There are several limitations in this research. First of all, a major limitation of the present study was the small patient cohort of different STTs. Furthermore, IVIM imaging is sensitive to little movement, which may be problematic for thigh IVIM imaging due to pulsation of arteries. Lastly, this study was only to screen out hemangioma from BSTTs, and further research is necessary to differentiate other types of STTs.

CONCLUSION

To our knowledge, this is the first of its kind report about the application of pixel-based IVIM imaging to evaluate heterogeneous STTs. It may provide useful information to discriminate malignant tumors from benign ones regarding patient stratification and strategy in further treatment.

REFERENCES

1. Radaelli S, Stacchiotti S, Casali PG, et al. Emerging therapies for adult soft tissue sarcoma. *Expert Rev Anticancer Ther.* 2014;14:689–704.
2. Lahat G, Lazar A, Lev D. Sarcoma epidemiology and etiology: potential environmental and genetic factors. *Surg Clin North Am.* 2008;88:451–481v.
3. Burningham Z, Hashibe M, Spector L, et al. The epidemiology of sarcoma. *Clin Sarcoma Res.* 2012;2:14.
4. Varma DG. Optimal radiologic imaging of soft tissue sarcomas. *Semin Surg Oncol.* 1999;17:2–10.
5. Theumann NH, Bittoun J, Goettmann S, et al. Hemangiomas of the fingers: MR imaging evaluation. *Radiology.* 2001;218:841–847.
6. Kransdorf MJ, Murphey MD. Radiologic evaluation of soft-tissue masses: a current perspective. *Am J Roentgenol.* 2000;175:575–587.
7. Pang KK, Hughes T. MR imaging of the musculoskeletal soft tissue mass: is heterogeneity a sign of malignancy? *J Chin Med Assoc.* 2003;66:655–661.
8. Le Bihan D. Intravoxel incoherent motion perfusion MR imaging: a wake-up call. *Radiology.* 2008;249:748–752.
9. Yabuuchi H, Matsuo Y, Kamitani T, et al. Parotid gland tumors: can addition of diffusion-weighted MR imaging to dynamic contrast-enhanced MR imaging improve diagnostic accuracy in characterization? *Radiology.* 2008;249:909–916.
10. Sumi M, Van Cauteren M, Sumi T, et al. Salivary gland tumors: use of intravoxel incoherent motion MR imaging for assessment of diffusion and perfusion for the differentiation of benign from malignant tumors. *Radiology.* 2012;263:770–777.
11. Le Bihan D, Turner R, MacFall JR. Effects of intravoxel incoherent motions (IVIM) in steady-state free precession (SSFP) imaging: application to molecular diffusion imaging. *Magn Reson Med.* 1989;10:324–337.
12. Lee EY, Yu X, Chu MM, et al. Perfusion and diffusion characteristics of cervical cancer based on intraxovel incoherent motion MR imaging-a pilot study. *Eur Radiol.* 2014;24:1506–1513.
13. Kallehauge JF, Tanderup K, Haack S, et al. Apparent diffusion coefficient (ADC) as a quantitative parameter in diffusion weighted

MR imaging in gynecologic cancer: dependence on b-values used. *Acta Oncol (Stockholm, Sweden).* 2010;49:1017–1022.

14. Lambregts DM, Maas M, Cappendijk VC, et al. Whole-body diffusion-weighted magnetic resonance imaging: current evidence in oncology and potential role in colorectal cancer staging. *Eur J Cancer (Oxford, England: 1990).* 2011;47:2107–2116.
15. Mueller-Lisse UG, Mueller-Lisse UL, Zamecnik P, et al. [Diffusion-weighted MRI of the prostate]. *Der Radiol.* 2011;51:205–214.
16. Tan CH, Wang J, Kundra V. Diffusion weighted imaging in prostate cancer. *Eur Radiol.* 2011;21:593–603.
17. Giannarini G, Petralia G, Thoeny HC. Potential and limitations of diffusion-weighted magnetic resonance imaging in kidney, prostate, and bladder cancer including pelvic lymph node staging: a critical analysis of the literature. *Eur Urol.* 2012;61:326–340.
18. Dyvorne HA, Galea N, Nevers T, et al. Diffusion-weighted imaging of the liver with multiple b values: effect of diffusion gradient polarity and breathing acquisition on image quality and intravoxel incoherent motion parameters – a pilot study. *Radiology.* 2013;266:920–929.
19. Le Bihan D, Turner R. The capillary network: a link between IVIM and classical perfusion. *Magn Reson Med.* 1992;27:171–178.
20. Lewin M, Fartoux L, Vignaud A, et al. The diffusion-weighted imaging perfusion fraction f is a potential marker of sorafenib treatment in advanced hepatocellular carcinoma: a pilot study. *Eur Radiol.* 2011;21:281–290.